Indoor Human Activity Recognition Based on Ambient Radar with Signal Processing and Machine Learning

Shangyue Zhu, Junhong Xu, Hanqing Guo, Qiwei Liu, Shaoen Wu
Department of Computer Science
Ball State University
Muncie, IN
{szhu,jxu7,hguo,qliu4,swu}@bsu.edu

Honggang Wang
Dept. of Electrical and Computer Engineering
University of Massachusetts Dartmouth
Dartmouth, MA
hwang1@umassd.edu

***Abstract*—Indoor human activity recognition has been extensively investigated. However, most of the solutions require sensors e.g. 9-axis IMU be equipped on human body or use image processing that presents privacy issues. This work proposes an ambient radar sensor based a solution to recognize the activities that humans normally perform in indoor environments. This solution uses a 7.8 GHz radar to emit 16 pulse signals every second and samples the reflected signals at 128 KHz to capture the fine dynamics of human activities. This solution designs a set of data preprocessing algorithms, including a data refining algorithm to filter outlier data, a contrastive divergence algorithm to remove background static reflection, and a transformation algorithm to convert the signal data into feature-rich spatial location changes. This solution also develops schemes to separate a collection of various activities into individuals. A lowpass frequency filter is designed to remove unwanted noisy data and the motion intensity is used to classify the activities into two high-level groups. It uses a slope-based approach and a k-means clustering to further finely recognize each activity. This solution has been extensively evaluated in a spacious research lab room and shows outstanding accuracy.**

I. Introduction

Indoor human activity recognition is crucial to many intelligent systems such as smart homes, smart health as well as smart security [2]. For instance, potential crash may occur when children jog or do some intense activities inside the home [1]. Elderly people have the potential to fall down when they try to stand up or sit down [2]. Hence, human activity recognition has been an active research area.

Many solutions have been proposed to recognize human activities. Some systems use camera videos and computer vision while many recent solutions are based on wearable sensors. However, camera based solutions have potential privacy issues [3]. Wearable based solutions result in inconvenience because the users have to remember to equip these sensors or devices such as smartphones. If they take off or forget the sensors or devices, the recognition voids. Thus, it is of ultimate interest to design a passive, non-invasive and ambient human activity recognition solution that does not present privacy concerns.

In this paper, we propose a solution of indoor Human Activity Recognition based on Ambient Radar sensors, *HARAR*. This work considers four types of indoor activities: *sit-to-stand, stand-to-sit, walking* and *jogging*. It has the following highlights:

- it uses miniature radar to emit signals at 16 pulse per second while the measurement of the reflected signal occurs at a very high frequency of 128 KHz to capture very fine dynamics of activities.
- it proposes a chain of signal processing algorithms to: 1) remove the exceptional measurement and interpolate the replacement, 2) filter out the static background reflections to keep only the motion reflections, and 3) transform the signal data into relative location changes with rich features.
- it designs: 1) an algorithm to separate the sequence of activity mixture into individual activities, 2) a lowpass filtering algorithm to remove the unwanted noisy components in the data for accuracy, and 3) a motion intensity based classification method to separate *sit-to-stand* and *stand-to-sit* from *walking* and *jogging*.
- it invents two features: slope gradient and relative velocity to recognize each activity finely with the k-means machine learning algorithm.

In the remaining, a brief overview of the human activity recognition and related work are presented in Section II. Our proposed solution is detailed in the Section III including the data preprocessing, coarse activity classification and fine activity recognition. Section IV presents our validation and verification of each key component of the solution and the overall performance evaluation of the entire system. Finally, Section V concludes this work.

II. Related Work

A. Human Activity recognition

Human activity recognition has been investigated for many smart home applications e.g. motion detection [4], [5]. Literature solutions have used various sensors, such as accelerometers [6], Gyroscope [7], light sensors [8], temperature sensors [9], videos [10], [11], etc. There sensors become a rich data

source of human objects' life. For instance, wearable sensors have been used for physiological states, such as step changes, moving directions, speed, etc [4], [6], [12].

Based on the data from various sensors, many algorithms have been proposed to recognize human activities [13]–[15]. Yan, et al, designed a multitask clustering algorithm to recognize activities with motion features derived from mobile images [14]. Dixit and Naik investigated some prediction algorithms to predict the next event to happen [15]. Their episode discovery algorithm was designed to find the frequency of occurrence of particular events.

B. Radar sensor

Radar sensor has been used in the military for long in detecting flight objects, but it has been recently considered for interactive systems and applications, because it does not depend on lighting, noise or atmospheric conditions [16], [17]. Google ATAP team has designed an mm-wave radar system Soli based on 60 GHz signals to capture subtle motions in finger gestures [18]. Soli emits signals at very high frequencies, samples the reflected signals at KHz frequencies, then use signal processing techniques to extract features, and employs machine learning to recognize different finger gestures with classification algorithms. Yavari, et al, investigate the use of Doppler radar sensor for occupancy monitoring [19].

III. System Design

To enable smart environments with commodity ambient sensors, we propose a solution: Human Activities Recognition Based on Ambient Radar (*HARAR*). *HARAR* repeats emitting a 7.8 GHz wireless radio signal about every 0.7 second through a sending antenna. Meanwhile, it actively measures the signal power reflected by human body parts with an array of receiving antennas. It then employs signal processing and machine learning methods to accurately recognize human activities based on the patterns of reflected signal power. We present the detail system design of *HARAR* in this section, including (a) data collection and (b)human activity recognition.

A. Sensing Platform, System Model and Data Collection

HARAR uses a continuous-wave radar sensing platform to collect human activity data by following the radar principles [2]. In particular, this sensing platform is based on Walabot[1] that has a size of 72 mm $\times$ 140 mm. Walabot supports multiple antenna pairs to sense a target area and each pair consists of two directional antennas working on different frequency ranges. FCC regulates the wireless operates over 3.3-10.3 GHz range. The average transmission power of both models is about -16 dBm. In this research, in order to simulate an ordinary home circumstance, we configure antennas to work on a medium frequency 7.85GHz. The radar field of the view is approximately 60 degrees horizontally and 15 degrees vertically.

Our radar sensing platform emits probing pulse signals $x(t)$ at a pulse repetition frequency (PRF) of 16 Hz, but within each pulse repetition interval (PRI), the receiver antenna samples the received signal $y(t)$ at a very high frequency of 8 KHz. Considering human activities usually stay on lower frequencies, such a radar sensing is capable enough to catch activity dynamics. Although Walabot provides APIs to get preprocessed data at coarse resolutions, it does provide a mechanism to extract raw received signal amplitudes at its native analog-to-digit (ADC) rate, which offers the highest resolution of data. Our system exactly uses this raw data option to obtain the highest possible resolution data of signal variation dynamics during human activities.

When a human object is within the detection area, body parts can be modeled as a collection of reflective points, as shown on Figure 1. The emitted signal $x(t)$ arrives at and is then modulated by body parts independently. As a result, the radar signal signature $y(t)$ at a receiver antenna is a mixture of those modulated signals. The posture changes of body parts in various activities are expected to result in different patterns in the radar signal signatures. Therefore, by analyzing the radar signal signature patterns, activities are expected to be recognized.

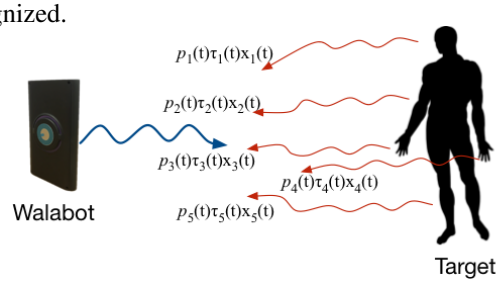

Fig. 1: Radar Sensing

We model the radar frequency response of human activities as a superposition of responses from a collection of N various discrete body scattering points, which can be formulated as:

$$y(t) = \sum_{0}^{N-1} \rho_i(t) r_i(t) x(t) \tag{1}$$

where $\rho_i(t)$ is the complex reflectivity parameter of the body reflective point i, $r_i(t)$ presents the corresponding round-trip channel response between the radar sensor and the body reflective point i.

It should be noted that the received signal $y(t)$ contains not only reflections from body parts, but also those from environment background. We define background reflections as "noise" $n(t)$ to the activity signals. Then $y(t)$ follows:

$$y(t) = \sum_{0}^{N-1} \rho_i(t) r_i(t) x(t) + n(t) \tag{2}$$

As the received signal signature $y(t)$ carries the information of body activities, we use its amplitude $|y(t)|$ as the data to drive our activity recognition and analytics. Based on the radar principle, we define two types of windows: *short window* and *long window*. A long window is composed of a number of short windows each of which consists of n consecutive samples of $|y(t_i)|$. The short window size n is empirically

[1]https://walabot.com/community

determined and it should be small enough to capture significant body part movements in an activity. We denote the data in the short window k as $A_k = (|y_{k0}(t)|, |y_{k1}(t)|, ...|y_{k(n-1)}(t)|)$, and the data of a long window S as $S = (A_0, A_1, ...A_l)$. In particular, our solution has the short window consisting of 500 consecutive measurements of $|y(t)|$. The long window spans an PRI consisting of 16 short windows for 8,000 measurements in total. Therefore, we have the short window data $A_k = (|y_{k0}(t)|, |y_{k1}(t)|, ...|y_{k(499)}(t)|)$, and the long window data $S = (A_0, A_1, ...A_{15})$.

B. Human Activity Recognition

With radar signal data collected and formatted into short and long windows, the activity recognition of *HARAR* is perfomed with three core modules: (1) data preprocessing that extracts the signal $\sum_0^{N-1} \rho_i(t) r_i(t) x(t)$ reflected by human body parts from the received signal mixture with noise, or namely filters out the background noise $n(t)$ from $y(t)$, (2) coarse activity classification that categorizes preprocessed signals into two groups: high-frequency and low-intensity activities, with a lowpass filter algorithm, and (3) fine activity recognition that recognizes specific activities in each group. The recognition procedure is illustrated as in Fig. 2.

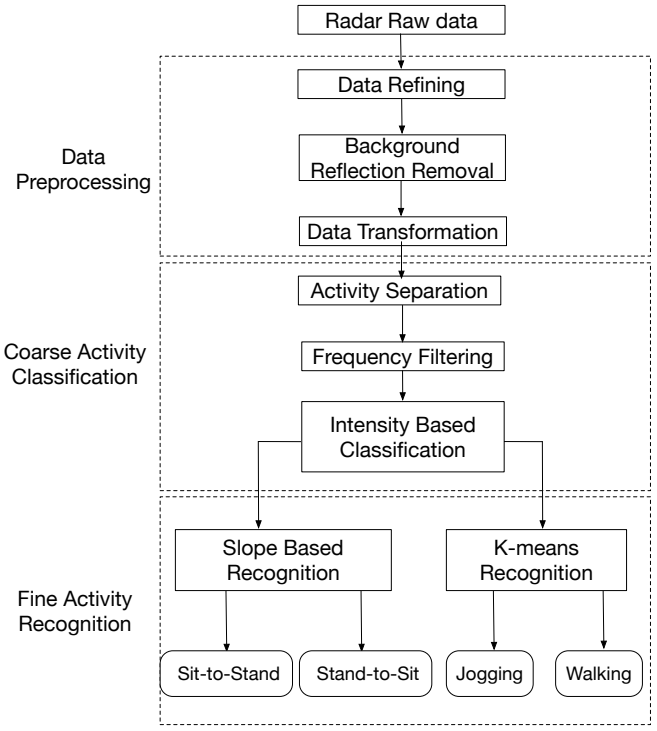

Fig. 2: Block diagram of the system design

1) Data Preprocessing: After raw measurements of $y(t)|$ are obtained, these data pass through a chain of signal processing blocks that: 1) filter out the background noise from the received mixture measurements, 2) remove exceptional measurements, and 3) transform the data for feature extraction.

Data Refining: The collected radar signal data is noisy because of: (1) the irregular surfaces of static objects in a background environment, (2) unexpected other signals, and (3) the imperfect mechanical capabilities e.g. reliability, stability, accuracy and resolution of the off-the shelf device.

The first step of the data preprocessing is to remove those exceptional data in each short window. In our platform, the transmitted radar signal has an upper bound amplitude. After the path loss and multi-path fading, the amplitude of the received radar signal $y(t)$ should be less than that of the transmitted signal $x(t)$. Namely this follows: $|y(t)| < |x(t)|$. Therefore, our algorithm removes a measurement $|y_i(t)|$ if $|y_i(t)| \geqslant |x(t)|$. To keep the same number of measurements in each short window, an interpolated measurement is needed. In our solution, the removed measurement is replaced by the mean of its previous and next measurements: $y_i = mean(y_{i-1}, y_{i+1})$.

Background Reflection Removal: Even after the exceptional data are removed, measurements contain both the signal reflected by body parts and by a background environment. One important observation is that, since a background environment is static, there should be no change on its reflection in different radar signal intervals. Namely, the variations of measurements across short or long windows should be only incurred by human body activities. Based on this observation, we design a contrastive divergence algorithm [20] to remove the background reflected signal and keep only reflections by body parts.

As shown in Equation (4), the contrastive divergence algorithm first calculates the divergence of all measurements between every two consecutive short windows, namely $|A_{k+1} - A_k|$, and then identifies and denotes the maximal divergence with its index i as D_i, which indicates the activity results in a signal variation peak at the i-th measurement in a short window.

$$D_i = max(|A_{k+1} - A_k|) \tag{3}$$

$$= max(|A_{k+1}[0] - A_k[0])|, ..., |A_{k+1}[n-1] - A_k[n-1]|) \tag{4}$$

Data Transformation: After the activity is captured with the maximal divergence D_i by the contrastive divergence algorithm, we only know its occurrence at a certain measurement moment in a particular short window. To recognize various activities, it is necessary to gain the knowledge of *how the location (namely the occurrence moment) of the maximal divergence D temporally changes across a sequence of short windows*. It is the pattern of the temporal location change of D that indicates various activities. We will use this information across the short windows in each long window S for activity recognition.

It is difficult to obtain the temporal location change of D. We rather transform the temporal location change of D across short windows to a relative *spatial* location change L, which, based on wireless propagation, is defined as:

$$L_i = |I_i - I_0| \times c/2 \tag{5}$$

where I_i and I_0 respectively represent the occurrence indice of D in the i-th and the first short window in a long window,

c is the speed of light, and the division by 2 is due to the radar signal round-trip propagation.

The transformation outcome is a vector M of a long window S, which records maximal divergence D and its relative spatial locations across a sequence of short windows. Suppose each long window S contains n short windows. M has a format as:

$$M = \begin{bmatrix}(D_0, L_0) & (D_1, L_1) & \cdots & (D_{n-1}, L_{n-1})\end{bmatrix} \quad (6)$$

2) Coarse Activity Classification: With the preprocessed data M across long windows, we further process the data to extract the high-level activity features, which includes (1) identifying individual activity occurrences, and (2) extracting body activity frequencies for each activity.

Activity Separation: With a period of time T modulated into a number of long windows $(S_0, S_1...)$, the activities occurring over the time period T can be separated with the data $(M_0, M_1...)$ over the long windows $(S_0, S_1...)$. Observing that between two activities there is only static "silent" background environment that results in 0 for the maximal divergence D, the activities are thus separated by a streak of "0"s in M. We define the activity length as a time-span T_{span} of the activity:

$$T_{span} = t_{end} - t_{start} \quad (7)$$

where t_{end} denotes the time when the activity ends, and t_{start} denotes the time when the activity starts. For instance, if an M has the data of (0, 0, D_i, D_{i+1}, D_{i+2}, $\cdots$, D_n, 0, 0), the time of D_i is counted as t_{start}, and the time of D_n is t_{end}. The time-span T_{span} is used to indicate a single complete activity phase. Then, deep features will be extracted over each T_{span} for the activity recognition.

Frequency Filtering: From frequency domain perspectives, human activities normally occur at low frequencies. For example, walking or running at certain velocities that cannot be as fast as a car, standing or sitting falling into a motion speed and acceleration range that are relatively small [22]. To further improve the recognition accuracy, we use a lowpass filter, Butterworth filter (BWF) algorithm [21], to remove all unwanted components from the preprocessed data and keep only the human activity data for the recognition. BWF filter focuses on eliminating noises and keeping fundamental activity motion information. It works as:

$$H(\omega)^2 = \frac{{G_0}^2}{1 + (\frac{\omega}{\omega_c})^{2n}} \quad (8)$$

where ω_c denotes cutoff frequency, ω denotes the input frequency. G_0 denotes the DC gain (the gain at zero frequency), which is a constant, and n represents the order of filter. The output $H(\omega)^2$ denotes the gain of the BWF working on the signal of frequency ω. After the cutoff frequency ω_c is set, the processed signal data contains only those frequencies less than or equal to ω_c.

In our solution, the vectors M of each separated activity are the input data to the BWF filter. The cutoff frequency ω_c is determined according to the research outcomes on frequency and velocity of people walking [22].

Intensity Based Classification: In activities: *sit-to-stand, stand-to-sit, walking,* and *jogging*, *sit-to-stand* and *stand-to-sit* obviously do not result in as much intensity as *walking* and *jogging* do. Therefore, they expect to incur much smaller relative spatial location changes L than those of *walking* and *jogging*. Therefore, the output of our BWF algorithm is classified into two categories: *low-intensity activities* and *high-intensity activities* based on their relative spatial location changes L. From our extensive tests, L=1.0 is the best threshold to differentiate these two categories. The fine activity recognition within these two categories is then performed by exploiting deep features as described next.

C. Fine Activity Recognition

After activities into two categories upon the motion intensity in the data, the final activity recognition is performed within each class.

1) Low-Intensity Activity Recognition: The low-intensity activities includes *sit-to-stand* and *stand-to-sit*. From the numerous measurements in these two activities, we have observed that *they result in two opposite slopes in the relative spatial location changes* L as defined in Equation (5): *ascending* and *descending*. This is because, no matter how the radar sensor is deployed, these two activities result in either the body approaching to the sensor or departing from the sensor in the space. In our system where the sensor is deployed on a desk that faces to the upper body portion, *sit-to-stand* generates an approaching style leading to a descending slope in L while *stand-to-sit* incurs an ascending slope.

The slope detection is performed as follows. These activities are first separated and extracted over a sequence of long windows with the time spanning algorithm in Equation 7. As a result, each T_{span} contains an activity of either *sit-to-stand* or *stand-to-sit*. Since the slope of each activity can be only either ascending or descending, the slope is determined according to the relative spatial location changes L in the T_{span}.

2) High-Intensity Activity Recognition: For high-intensity activities *walking* and *jogging*, they obviously differ in motion velocity. Thus, we use the velocity as the key feature to differentiate them. Reasonably assuming the velocity of the body does not change widely within a few of long windows, with the observation that the motion results in contrastive divergence D occurring at various indices in a sequence of long windows, the velocity V_i in the i-th long window of an activity follows:

$$V_i \propto \frac{1}{|I_i - I_{i-1}|} \quad (9)$$

where I_i is the maximal contrastive divergence occurring index in the long window. Therefore, rather than getting the actual velocity, we use $|I_i - I_{i-1}|$ as a "relative velocity" to represent the actual velocity in recognition. After we obtain the velocity, we then use k-means classification algorithm to different the *walking* and *jogging* activities.

IV. Performance Evaluation

We have extensively evaluated the performance of our *HARAR* in a real environment.

A. Experiment Setting

The experiments have been performed in the Intelligent Computing and Communication Systems research lab RB305 at Ball State University. The lab room has a "L" shape with 10 desks and some other furnitures such as chairs and cabinets. This room has a wide space to allow people to perform test activities as in regular life. Figure 3 shows the deployment of the test platform in a part of the room. In *sit-to-stand* and *stand-to-sit*, the human object is 2m away from the radar sensor. In *walking* and *jogging*, the human object moves up to 5m from the radar sensor.

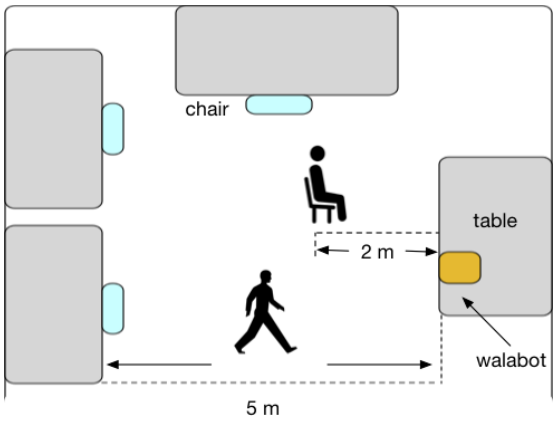

Fig. 3: Experiment Setting

B. Activity Detection and patterns

The first evaluation is to verify the effectiveness of *HARAR* in detecting human body motions and forming activity patterns. In the experiments, the human objects have performed each of those four activities for 30 seconds. During *walking* and *jogging*, the human objects move back and forth. To magnify the details, we have selected the data of the first 150 out of about 430 long windows in each activity. The results are plotted in Figure 4, where y-axis of all sub-figures represents the received signal power level in the scale of the radar, and x-axis tells the long window number. It can be observed that (1) *sit-to-stand* and *stand-to-sit* both result in clearly lower frequencies and received power levels than *walking* and *jogging*, and (2) the data of *walking* and *jogging* seems continuous while *sit-to-stand* and *stand-to-sit* are bursty.

C. Coarse Activity Classification

This experiment evaluates the effectiveness of using the BWF frequency filter algorithm and the motion intensity to classify the activities into two coarse categories. The BWF filter algorithm has been applied to the entire 430 preprocessed activity data in each activity that are collected in the experiments in Section IV-B. The cutoff frequency ω_c is loosely set to 3.3 Hz to allow the activity frequencies are captured safely. The results of four activities are illustrated in Figure 5 where y-axis still refers to the relative spatial location change L. From the frequency domain analysis, *sit-to-stand* and *stand-to-sit* have peak frequencies smaller than 3 Hz while those of

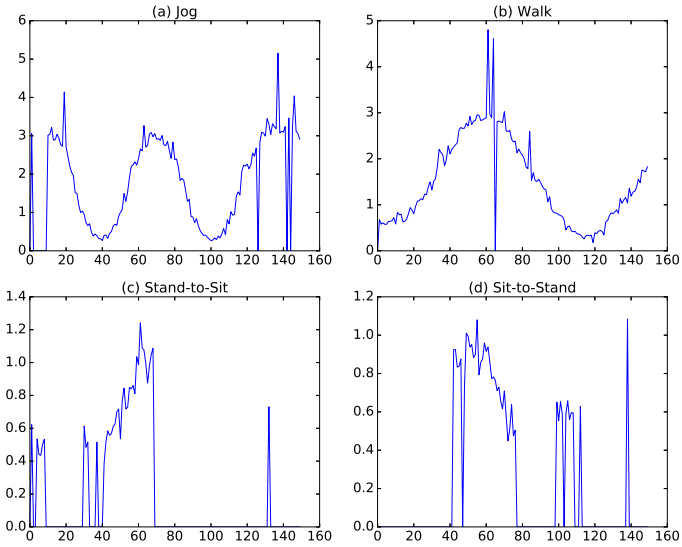

Fig. 4: Activity Detection and Patterns

walking and *jogging* are larger than 3 Hz. Meanwhile, *walking* and *jogging* have mostly resulted large relative spatial location changes (0.5, 3) on the y-axis while *sit-to-stand* and *stand-to-sit* have the values smaller than 1.0. This meets the expectation and analysis in Section III-B2.

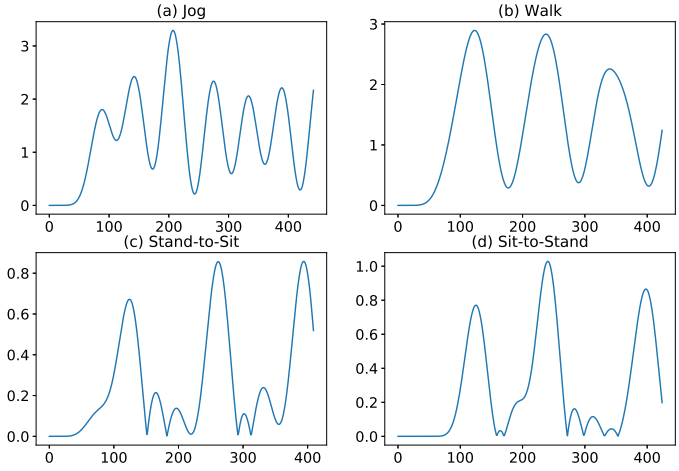

Fig. 5: BWF Frequency Filtering on Activity Data

D. Fine Activity Recognition

We have then performed experiments to evaluate the effectiveness of fine activity recognition algorithms in each coarse activity group.

1) Low-Frequency Activities: In this experiment, the human objects have continuously performed seven *sit-to-stand* and six *stand-to-sit* activities. The data has been first preprocessed to generate the relative spatial location changes L over long windows, which is plotted on the left in Figure 6. We have then used the time spanning algorithm as in Section III-B2 to separate activities, and the slope detection algorithm in Section III-C1 to determine the activity is *sit-to-stand* or *stand-to-sit*. As a result, *HARAR* can accurately recognize those seven *sit-to-stand* and six *stand-to-sit* activities.

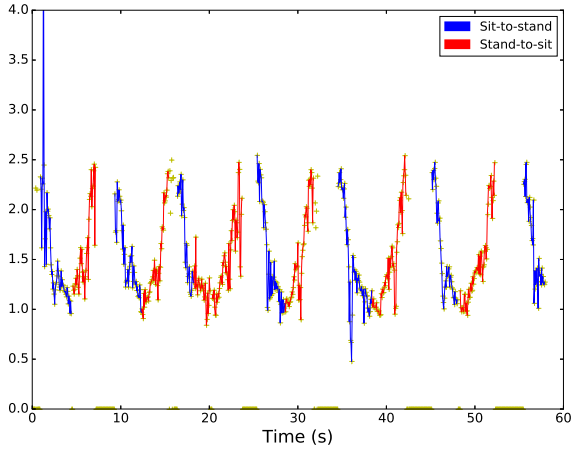

Fig. 6: Relative spatial locations of low-frequency activities

2) High-Frequency Activities: In this experiment, the human objects have walked back and forth at random speeds in one minute and then jogged for another minute. After preprocessing, we have calculated the relative velocities as in Section III-C2, which is plotted in Figure 7 with 880 data points where the dots in blue are from *jogging* and red dots are from *walking*. We can observe that the relative velocity clearly shows advantages in differing these two activities.

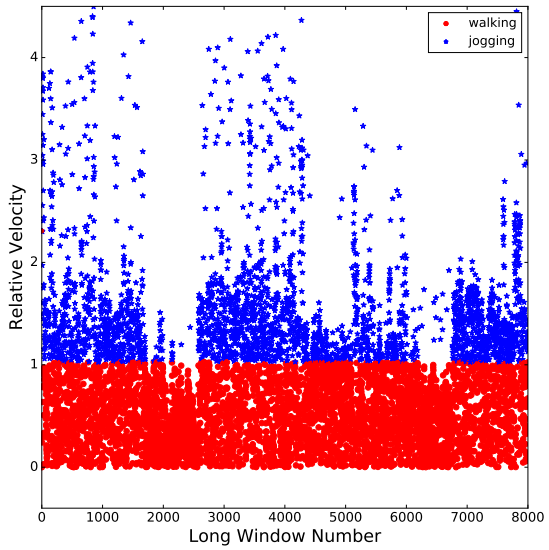

Fig. 7: Relative velocity of high-frequency activities

E. Accuracy

Finally, we have evaluated the prediction accuracy of *HARAR* in activity recognition. We have performed all four types of activities totally for 80 tests: 23 walkings, 20 joggings, 17 sit-to-stands and 20 stand-to-sits. Each activity has lasted for 60 seconds. All the data have been mixed together and preprocessed. Then they are passed in the frequency filtering and classified into two coarse categories. Then the final recognition has been performed in each category. The recognition between *walking* and *jogging* is performed with k-means algorithm based on the relative velocity as in Section III-C2. The results are shown in Table I. The accuracies for *walking, jogging, sit-to-stand*, and *stand-to-sit* are respectively: 82.6%, 95%, 82.3%, and 80%. The overall accuracy is 85%. The performance seems not very high, but it is outstanding with only the radar sensor without extra equipment.

TABLE I: Prediction Accuracy

Recognized/Actual	walking	jogging	sit-to-stand	stand-to-sit
walking	19	1	0	0
jogging	1	19	0	0
sit-to-stand	2	0	14	4
stand-to-sit	1	0	3	16

V. Conclusion

In this work, we propose a radar-based indoor human activity recognition solution, *HARAR*. This solution avoids the inconvenience of many literature solutions that requires sensors be installed on human bodies. *HARAR* measures the human activities with radar signals at very high frequency sampling to capture activity dynamics. Window-based signal processing algorithms are designed to remove background environment noise. A set of features are designed in *HARAR* to recognize the activities. The extensive evaluations demonstrate that *HARAR* can achieve an accuracy of 85%.

References

[1] Jun Goto, Takuya Kidokoro, Tomohiro Ogura, and Satoshi Suzuki. Activity recognition system for watching over infant children. In *RO-MAN, 2013 IEEE*, pages 473–477. IEEE, 2013.

[2] Branka Jokanovic, Moeness Amin, and Fauzia Ahmad. Radar fall motion detection using deep learning. In *Radar Conference (RadarConf), 2016 IEEE*, pages 1–6. IEEE, 2016.

[3] Yoshifumi Nishida, Toshio Hori, Shin-ichi Murakami, and Hiroshi Mizoguchi. Minimally privacy-violative system for locating human by ultrasonic radar embedded on ceiling. In *Systems, Man and Cybernetics, 2004 IEEE International Conference on*, volume 2, pages 1549–1554. IEEE, 2004.

[4] Xing Su, Hanghang Tong, and Ping Ji. Activity recognition with smartphone sensors. *Tsinghua Science and Technology*, 19(3):235–249, 2014.

[5] Miss Sapana K Mishra, Faizpur JTMCOE, and KS Bhagat. A survey on human motion detection and surveillance. *International Journal of Advanced Research in Electronics and Communication Engineering (IJARECE) Volume*, 4, 2015.

[6] Subhas Chandra Mukhopadhyay. Wearable sensors for human activity monitoring: A review. *IEEE sensors journal*, 15(3):1321–1330, 2015.

[7] Stefan Dernbach, Barnan Das, Narayanan C Krishnan, Brian L Thomas, and Diane J Cook. Simple and complex activity recognition through smart phones. In *Intelligent Environments (IE), 2012 8th International Conference on*, pages 214–221. IEEE, 2012.

[8] Uwe Maurer, Asim Smailagic, Daniel P Siewiorek, and Michael Deisher. Activity recognition and monitoring using multiple sensors on different body positions. In *Wearable and Implantable Body Sensor Networks, 2006. BSN 2006. International Workshop on*, pages 4–pp. IEEE, 2006.

[9] Tanzeem Choudhury, Sunny Consolvo, Beverly Harrison, Jeffrey Hightower, Anthony LaMarca, Louis LeGrand, Ali Rahimi, Adam Rea, G Bordello, Bruce Hemingway, et al. The mobile sensing platform: An embedded activity recognition system. *IEEE Pervasive Computing*, 7(2), 2008.

[10] Jay Prakash Gupta, Pushkar Dixit, and Vijay Bhaskar Semwal. Analysis of gait pattern to recognize the human activities. *IJIMAI*, 2(7):7–16, 2014.

[11] Ahmad Jalal and Shaharyar Kamal. Real-time life logging via a depth silhouette-based human activity recognition system for smart home services. In *Advanced Video and Signal Based Surveillance (AVSS), 2014 11th IEEE International Conference on*, pages 74–80. IEEE, 2014.

[12] Piyush Gupta and Tim Dallas. Feature selection and activity recognition system using a single triaxial accelerometer. *IEEE Transactions on Biomedical Engineering*, 61(6):1780–1786, 2014.

[13] Sajal Das and Diane Cook. Designing smart environments: A paradigm based on learning and prediction. *Pattern Recognition and Machine Intelligence*, pages 80–90, 2005.

[14] Yan Yan, Elisa Ricci, Gaowen Liu, and Nicu Sebe. Egocentric daily activity recognition via multitask clustering. *IEEE Transactions on Image Processing*, 24(10):2984–2995, 2015.

[15] Aditi Dixit and Anjali Naik. Use of prediction algorithms in smart homes. *International Journal of Machine Learning and Computing*, 4(2):157, 2014.

[16] Qian Wan, Yiran Li, Changzhi Li, and Ranadip Pal. Gesture recognition for smart home applications using portable radar sensors. In *Engineering in Medicine and Biology Society (EMBC), 2014 36th Annual International Conference of the IEEE*, pages 6414–6417. IEEE, 2014.

[17] Youngwook Kim, Sungjae Ha, and Jihoon Kwon. Human detection using doppler radar based on physical characteristics of targets. *IEEE Geoscience and Remote Sensing Letters*, 12(2):289–293, 2015.

[18] Jaime Lien, Nicholas Gillian, M Emre Karagozler, Patrick Amihood, Carsten Schwesig, Erik Olson, Hakim Raja, and Ivan Poupyrev. Soli: Ubiquitous gesture sensing with millimeter wave radar. *ACM Transactions on Graphics (TOG)*, 35(4):142, 2016.

[19] Ehsan Yavari, Hsun Jou, Victor Lubecke, and Olga Boric-Lubecke. Doppler radar sensor for occupancy monitoring. In *Silicon Monolithic Integrated Circuits in RF Systems (SiRF), 2013 IEEE 13th Topical Meeting on*, pages 216–218. IEEE, 2013.

[20] Geoffrey E Hinton. Training products of experts by minimizing contrastive divergence. *Training*, 14(8), 2006.

[21] A Soltan Ali, Ahmed Gomaa Radwan, and Ahmed M Soliman. Fractional order butterworth filter: active and passive realizations. *IEEE Journal on emerging and selected topics in circuits and systems*, 3(3):346–354, 2013.

[22] Tianjian Ji et al. Frequency and velocity of people walking. *Structural Engineer*, 84(3):36–40, 2005.

[23] Jin Chen, Per Jönsson, Masayuki Tamura, Zhihui Gu, Bunkei Matsushita, and Lars Eklundh. A simple method for reconstructing a high-quality ndvi time-series data set based on the savitzky–golay filter. *Remote sensing of Environment*, 91(3):332–344, 2004.